Terahertz Imaging With Quantum-Well Photodetectors

T. Zhou, R. Zhang, X. G. Guo, Z. Y. Tan, Z. Chen, J. C. Cao, and H. C. Liu, *Fellow, IEEE*

***Abstract*— We present an imaging system based on a terahertz (THz) quantum-well photodetector (QWP). The THz QWP possessing high sensitivity at THz frequency band (0.3–10 THz) is utilized as a detector for imaging. We obtained images of a concealed sample in envelope by detecting the transmitted THz radiation from a black-body source as background radiation. This letter shows the potential of THz QWPs for imaging.**

***Index Terms*— Detector, imaging, quantum well, terahertz.**

I. Introduction

TERAHERTZ (THz) range radiation occupies a frequency band of about 0.3THz–10THz (corresponding wavelengths 1mm–30um), which has shown potential for applications in the fields of material characterizations, security screening and biomedical imaging. Research on imaging using THz radiation had undergone rapid development in the past few years. The first THz imaging of a leaf and a circuit was demonstrated in 1995 [1]. Thereafter THz imaging experiments on biological tissue for rat brain frontal sections and real-time imaging for mail screening and fingerprint identification were reported [2]-[4]. Active 3D THz imaging of computed tomography (CT) was performed to detect the inner structure of polystyrene models [5]. THz imaging is also potentially useful for situation awareness at a fire disaster, where smoke and dust particles exist, because scattering extinction coefficient in THz is much smaller than that at infrared wavelengths [6]. The detectors of the research mentioned above are mostly broad band detectors such as cryogenically cooled bolometers which are in general highly sensitive, but like all heat-based detection devices, they are intrinsically slow [7]. Additionally, coherent techniques like time-domain spectroscopy (TDS) possess a good sensitivity, but they are experimentally more complicated, expensive and difficult to integrate than incoherent ones [8]. As an extension of quantum well infrared photodetector into the THz, THz QWP is provided with characteristics of high sensitivity, narrow response range and fast photoresponse [9]-[12]. In this letter, we demonstrate the use of a THz QWP for imaging.

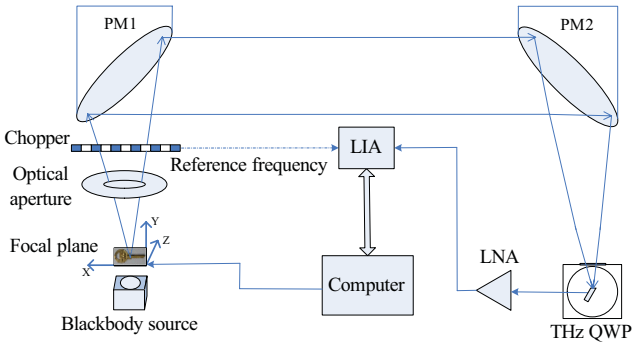

Fig. 1. Schematic of the THz imaging experimental setup.

II. Experimental Setup

The THz QWP in our experiment is a GaAs/AlGaAs multiple quantum well structure grown by molecular beam epitaxy, which consists of 23 modules made of 22.1nm GaAs wells and 95.1nm $Al_{0.015}Ga_{0.985}As$ barriers. The THz QWP operates at ~3.4K, peak at 3.2THz with a responsivity of 0.5A/W and reaches about 10^{11}cm. $Hz^{1/2}$/W in detectivity. (NEP about 8×10^{-13}W/$Hz^{1/2}$). The detector is placed on the cold finger of a close-cycle cryostat with a polyethylene window.

A schematic of the experiment is shown in Fig. 1. The sample is placed at the focal plane (X-Y plane) of an off-axis parabolic mirror (PM1) and mounted on a computer controlled X-Y translation stage. PM1 and PM2 have the same focal length of 10cm. In the front of the sample, we use an optical aperture to reduce the background noise. After a chopper, the emission is collected by PM1 and focused by PM2 onto the THz QWP through the polyethylene window

Manuscript received November 30, 2011; revised April 11, 2012; accepted April 14, 2012. Date of publication April 24, 2012; date of current version May 22, 2012. This work was supported in part by the 863 Program of China under Project 2011AA010205, in part by the 973 Program of China under Grant 2011CB925603, in part by the National Natural Science Foundation of China under Grant 61131006, Grant 60721004, Grant 11074266, and Grant 61176086, in part by the Major National Development Project of Scientific Instrument and Equipment under Grant 2011YQ150021, in part by the Important National Science and Technology Specific Projects under Grant 2011ZX02707, in part by the Major Project under Project YYYJ-1123-1, in part by the Hundred Talent Program of the Chinese Academy of Sciences, and in part by the Shanghai Municipal Commission of Science and Technology under Project 10JC1417000, Project 11ZR1444000, Project 11ZR1444200, and Project 09DJ1400102.

T. Zhou, R. Zhang, X. G. Guo, Z. Y. Tan, Z. Chen, and J. C. Cao are with the Key Laboratory of Terahertz Solid-State Technology, Shanghai Institute of Microsystem and Information Technology, Chinese Academy of Sciences, Shanghai 200050, China (e-mail: tzhou@mail.sim.ac.cn; rzhang@mail.sim.ac.cn; xgguo@mail.sim.ac.cn; zytan@mail.sim.ac.cn; zchen@mail.sim.ac.cn; jccao.@mail.sim.ac.cn).

H. C. Liu is with the Key Laboratory of Artificial Structures and Quantum Control (Ministry of Education), Department of Physics, Shanghai Jiao Tong University, Shanghai 200240, China (e-mail: h.c.liu@sjtu.edu.cn).

Color versions of one or more of the figures in this letter are available online at http://ieeexplore.ieee.org.

Digital Object Identifier 10.1109/LPT.2012.2196033

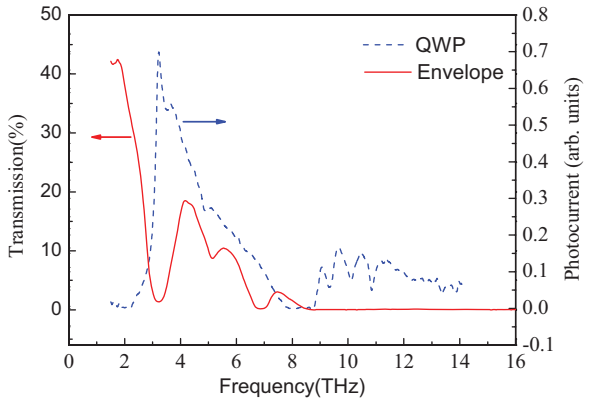

Fig. 2. Transmission spectrum of an envelope (red) in far infrared frequency band. The blue dashed line represents normalized photocurrent spectra of the THz QWP at a bias of 25 mV. The results are obtained on a Fourier transform spectrometer.

(thickness is 1.8mm) with a transmission of 75% at 3.2THz. The extracted voltage signal is amplified by a low noise amplifier (LNA). The amplified voltage is read out by a lock-in amplifier (LIA) which is controlled by a computer for synchronization with the X-Y stage.

III. Results and Discussion

We demonstrate THz imaging of a metal key in an envelope by using a blackbody source as background radiation. The experimental setup is as Fig. 1: we place the envelope (the key is fixed inside) at the focal plane of PM1 on the stage and the blackbody source is placed right behind the envelope along the optical axis. The blackbody source (BDB20A) is commercially available and the temperature range is set from room temperature (300K) to 473K in the experiment. The aperture of the blackbody source is set at 60mm in diameter to cover the scan region of the object. Small radiation area results in a too weak signal to be detected. The chopper frequency is set at 25Hz. The scan step of the sample is 1mm both in X and Y axes.

The photocurrent spectrum of the QWP and transmission spectrum of an envelope in far infrared frequency region are illustrated in Fig. 2. As we can see, the blue dashed line is normalized photocurrent spectra of the THz QWP which shows a peak at 3.2THz and a narrow response range from 3THz to 6THz where the envelope possesses a transmission more than more than 15% around 4.2THz, in mid infrared frequency region the transmission is zero. The narrow response helps to block out-of-band signals from environment. Although the signal is decreased by the envelope, it still can be extracted by the THz QWP because of its high detectivity.

Fig. 3(a) shows the responsive voltage of the THz QWP and SNR under the radiation of the black-body at different temperatures with an interval of 10K. The blackbody temperature could be controlled with an accuracy of 0.03K. We take SNR as spatially and temporally averaged signal <x> divided by the RMS noise σ, SNR = <x>/σ. Here, <x> represents average voltage at every temperature point and σ mainly characterizes noise from the detector and the circuit. We collect 20 data points of the responsive voltage to calculate

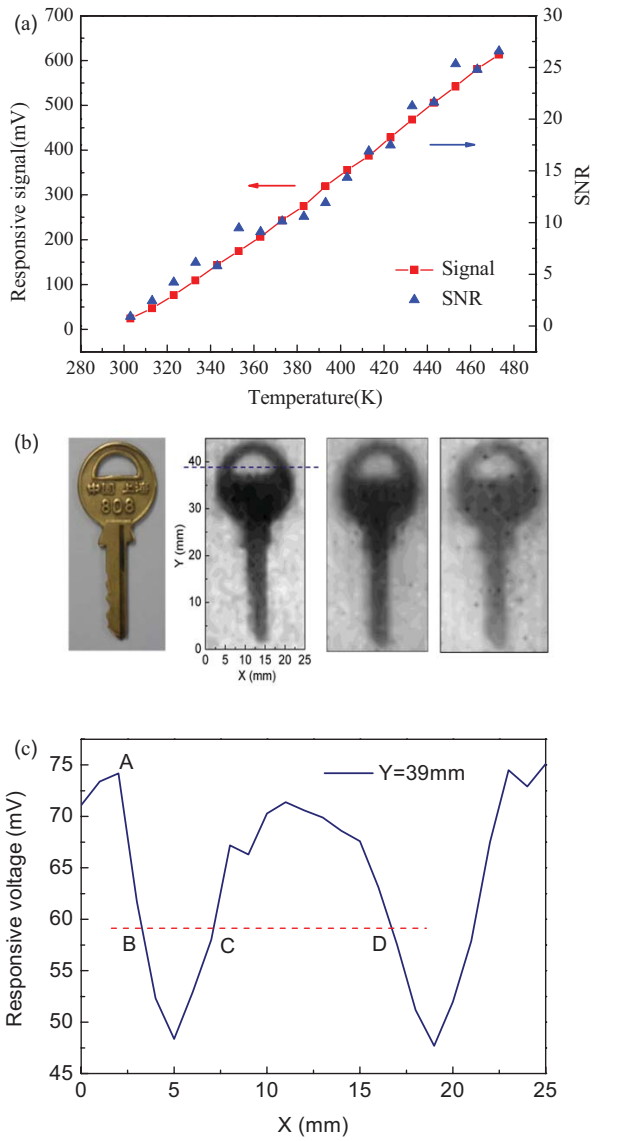

Fig. 3. (a) Responsive voltage of THz QWP and SNR versus temperature of the black-body source. The red square symbols represent experimental result at different temperature points with the interval of 10 K and the blue triangles represent calculated SNR at the temperature points. (b) Comparison of the hidden metal key between optical picture (left) and THz images with different SNR: 27, 17, and 10 (from left to right). For the images the highest transmission is shown in white and the lowest transmission is shown in black. (c) THz amplitude of a cross section of the image with SNR 27 in (b) and the blue dashed line indicates the location $Y = 39$ mm.

<x> and σ at every scan point, and find that the noise remains unchanged (at around 2mV) while the responsive voltage (red square) increases as temperature rises. The unchanged noise level is related to the fact that the detector is background limited, rather signal noise limited. The highest SNR values calculated are ~27 and ~300 with and without the envelope, respectively. The scan region is 25mm×45mm and the image consists of 1125 pixels with a spacing of 1mm between neighboring pixels. The total time of scanning takes about 30 min. The speed is mainly limited by the translation scan mechanism.

Fig. 3(b) presents 3 images under different SNR of 27, 17 and 10 corresponding to temperature of 473K, 423K

and 373K. As the SNR decreases the quality of the image becomes worse. The last image appears some black spots and the contour becomes fuzzy. It is mainly due to the signal loss during the transmission and noise of the system. To estimate the spatial resolution of the first THz image in Fig. 3(b), the transmission amplitude of a cross section at Y = 39mm (the blue dashed line) in the best image is drawn in Fig. 3(c). Because of the diffraction effect and the non-flat focal plane, when the signal crosses from "air" to the "key", the collecting area of signal on the focal plane changes, and consequently the transmission intensity does not drop to the minimum immediately. We choose half amplitude (red dashed line) as a threshold to estimate spatial resolution. Point A represents the transmission amplitude in this letter area, below the red dashed line it comes into the "key" area. The distance of point A and B represents the spatial resolution which is estimated 1∼1.2mm from the intensity line and we even could estimate the width of the key hole crossed. The distance between the points C and D represents the hole width which is 9.6mm as measured, the actual size is 9.2mm at this cross section.

IV. Conclusion

We have demonstrated THz imaging based on a THz QWP. As examples, we obtained images of a key in an envelope. This experiment has proved that imaging based on THz QWP is feasible. For real-time imaging a THz QWP focal plane array needs to be constructed.

References

[1] B. B. Hu and M. C. Nuss, "Imaging with terahertz waves," *Opt. Lett.*, vol. 20, no. 16, pp. 1716–1718, Aug. 1995.

[2] J. Darmo, *et al.*, "Imaging with a terahertz quantum cascade laser," *Opt. Express*, vol. 12, no. 9, pp. 1879–1884, May 2004.

[3] S. M. Kim, F. Hatami, and J. S. Harris, "Biomedical terahertz imaging with a quantum cascade laser," *Appl. Phys. Lett.*, vol. 88, no. 15, pp. 153903-1–153903-3, Apr. 2006.

[4] A. W. M. Lee, S. Kumar, B. S. Williams, Q. Hu, and J. L. Reno, "Real-time imaging using a 4.3-THz quantum cascade laser and a 320×240 microbolometer focal-plane array," *IEEE Photon. Technol. Lett.*, vol. 18, no. 13, pp. 1415–1417, Jul. 1, 2006.

[5] X. X. Yin, B. W.-H. Ng, J. A. Zeitler, K. L. Nguyen, L. F. Gladden, and D. Abbott, "Local computed tomography using a THz quantum cascade laser," *IEEE Sensors J.*, vol. 10, no. 11, pp. 1718–1731, Nov. 2010.

[6] N. Oda, "Uncooled bolometer-type terahertz focal plane array and camera for real-time imaging," *Compt. Rendus Phys.*, vol. 11, nos. 7–8, pp. 496–509, Oct. 2010.

[7] J. P. Rice, E. N. Grossman, and D. A. Rudman, "Antenna-coupled high-T_c, air-bridge microbolometer on silicon," *Appl. Phys. Lett.*, vol. 65, no. 6, pp. 773–775, Aug. 1994.

[8] R. E. Drullinger, *et al.*, "2.5-THz frequency difference measurements in the visible using metal-insulator-metal diodes," *Appl. Phys. Lett.*, vol. 42, no. 2, pp. 137–138, Jan. 1983.

[9] H. C. Liu, C. Y. Song, A. J. SpringThorpe, and J. C. Cao, "Terahertz quantum-well photodetectors," *Infr. Phys. Technol.*, vol. 47, nos. 1–2, pp. 169–174, Apr. 2005.

[10] H. C. Liu, H. Luo, C. Y. Song, Z. R. Wasilewski, A. J. SpringThorpe, and J. C. Cao, "Terahertz quantum well photodetectors," *IEEE J. Sel. Topics Quantum Electron.*, vol. 14, no. 2, pp. 374–377, Apr. 2008.

[11] R. Zhang, *et al.*, "Metal-grating-coupled terahertz quantum-well photodetectors," *IEEE Electron Device Lett.*, vol. 32, no. 5, pp. 659–661, May 2011.

[12] P. D. Grant, R. Dudek, M. Buchanan, and H. C. Liu, "Room-temperature heterodyne detection up to 110 GHz with a quantum-well infrared photodetector," *IEEE Photon. Technol. Lett.*, vol. 18, no. 21, pp. 2218–2220, Nov. 1, 2006.